論文 한국공작기계학회지 제 8 권 제 4 호 1999. 8.
Journal of the Korean Society of Machine Tool Engineers

STS 316의 시효 열화 처리와 크리프 거동 특성

임지우* · 임병수**

Thermal Aging and Creep Rupture Behavior of STS 316

Ji Woo Im* · Byeong Soo Lim**

Abstract

Although type 316 stainless steel is widely used such as in reactors of petrochemical plants and pipes of steam power plants, and is attracting attention as potential basic material for the fast breeder reactor structure alloys in nuclear power plants, the effect of precipitates which form during the long term exposure at service temperature on creep properties is not known sufficiently. In this study, to investigate the creep properties and the influence of prior aging on the microstructure to form precipitates, specimens were first solutionized at 1130℃ for 20 minutes and then aged for different times of 0 hr, 100 hrs, 1000 hrs and 2200 hrs at 750℃. After heat treatments, tensile tests both at room temperature and 650℃ and constant load creep rupture tests were carried out.

Keywords : Creep Rupture(크리프 파단), STS 316(316 스테인리스강), Thermal Aging Treatment(열적 시효 처리), Creep Stress Exponent(크리프 응력 지수), Creep Activation Energy(크리프 활성화 에너지).

INTRODUCTION

Generally, metallic materials are crept at a homologous temperature (the ratio Ta/Tm, where Ta is the temperature under consideration and Tm is the melting temperature) greater than 0.4. A number of equipments that operate in power plants, petrochemical plants, oil refineries and airplanes are exposed to the creeping temperature.

At creep condition, because of high temperature, microstructures of the structure alloys change continuously, and this change influences the creep property. Lot of studies have been reported on the effect of microstructure on creep and stress rupture behavior, which is associated with the grain size[1,2] and precipitates[3]. Particularly, studies which are associated with the precipitation behavior consist of matching fracture types to precipitates by means of long term creep rupture test[4~6], and investigating effects of precipitates on creep behavior by means of prior aging treatment[7]. But, studies by the long term creep rupture tests are localized on the fracture surface, and most studies by prior aging treatment are of short term, and therefore, they do not reflect the precipitation behavior that happens to long time service equipments at high temperature sufficiently.

In this study, the effect of long term aging

*성균관대학교 대학원 기계설계학과
**성균관대학교 기계공학부 교수

treatment on creep behavior in type 316 stainless steel which is widely used in high temperature equipments such as pipes of steam power plants and reactors of petrochemical plants was investigated. At service temperature of these equipments, the most important change of microstructure in type 316 stainless steel is the precipitation of cabides and intermetallic compounds. Therefore, the purpose of this study is to investigate effects of the precipitate such as carbide with respect to the aging time of up to 2200 hrs at 750℃ on the creep rupture behavior using the solutionized 316 stainless steel. This kind of investigation on the change of microstructure by precipitation is indispensable to not only safe design but also the estimation of life and efficient service of high temperature equipments.

EXPERIMENTAL PROCEDURES

Test Specimens and Equipment

Table 1 shows the chemical composition of the hot rolled type 316 stainless steel used in the study. Before the aging treatment, all specimens were solutionized at 1130℃ for 20 minutes in order to resolve precipitates which may exist into the matrix of austenite, and subsequently water quenched in order to avoid the carbide precipitation at the grain boundary during the cooling process. After the solution treatment, specimens were aged for different times of 0 hr, 100 hrs, 1000 hrs and 2200 hrs at 750℃. The aging temperature is determined by the TTP (Time-Temperature-Precipitation) diagram of type 316 stainless steel[8], according to which, the typical precipitates that develop during the service, form fastest at 750℃.

For heat treatments of all specimens, a box type electric resistance furnace(Lindberg type 51442) was used, and a K type thermocouple was attached to the specimen for temperature control. The temperature was controlled with the accuracy of ±1.5℃. Tensile properties were measured at room temperature and 650℃ with 10 ton capacity hydraulic servo material test system (Shimadzu EF 0112-32) according to ASTM E8 and E21 using KS B 0810-14A type specimen(Fig.1). A 3 zone type electric resistance furnace was used to maintain the temperature during the measurement.

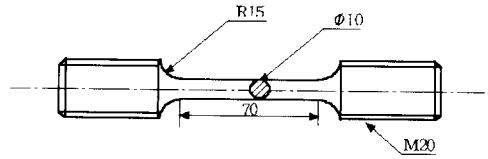

Fig. 1. Geometry of tension specimen.

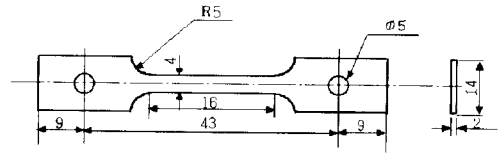

Fig. 2. Geometry of creep rupture specimen.

Creep rupture tests were conducted with a 3 ton capacity dead weight type constant load creep test(Shinwon SW-CFT3) according to ASTM E139. Fig. 2 shows the shape of the specimen. The displacement was measured using LVDT(Kyowa DT-50A) system and the signal was amplified with signal conditioner (Instech SM-10) and recorded on PC using data acquisition system. The strain was calculated according to ASTM E139.

Experimental Condition

After the aging treatment, the microstructure was examined with an optical microscope and the grain size was measured to investigate the effect of the aging treatment on the grain size. To examine the microstructure, the etchant of Gryceregia which etches precipitates selectively was used.

Constant load creep rupture tests were

Table 1. Chemical composition of STS 316(wt.%)

C	Si	Mn	P	S	Ni	Cr	Mo	Fe
0.046	0.58	1.04	0.020	0.005	10.55	16.59	2.10	rem

conducted under different stresses of 210, 230, 250 and 270MPa at 650℃. Under 230MPa, tests were conducted at three temperatures of 650℃, 675℃ and 700℃.

RESULTS AND DISCUSSIONS

Microstructure and Tensile Test

Table 2 shows grain size and hardness of each aged specimen. The change in grain size against the aging time was negligible, however, a significant increase in hardness in the 1000 hr and 2200 hr aged specimens was noted, which is believed to be the result of well dispersed carbides in the grain and at the grain boundaries. Table 3 shows tensile properties of the each aged specimen.

At room temperature, both tensile and yield strengths of 1000 hr aged specimen were the greatest, with the least ductility value. However, there was not much difference between 1000 hr and 2200 hr aged specimens. At 650℃, 2200 hr aged specimen showed the greatest value in yield and tensile strength, however, again, there was not much difference between 1000 hr and 2200hr aged specimens.

Fig. 3 shows optical microstructures of each aged specimen. As the etchant Glyceregia etches precipitates preferentially, Fig. 3a shows only some parts of grain boundaries, indicating onlyfew precipitates form at the grain boundaries. Fig. 3b which is the microstructure of 100 hr aged specimen at 750℃ shows carbides at the

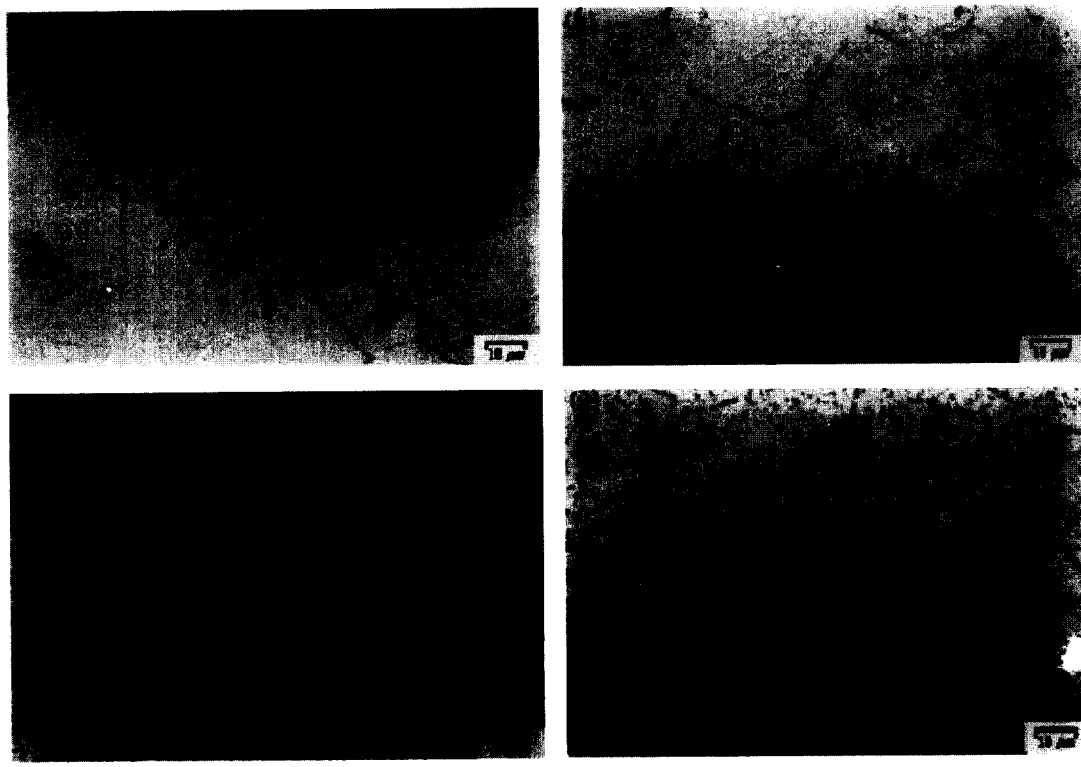

Fig. 3. Light optical microstructures of each aged specimen.
(a) not aged. (b) 100 hr at 750℃. (c) 1000hr at 750℃.
(d) 2200hr at 750℃. (etchant : Glyceregia)

Table 2. Grain size and hardness of each aged specimen

Aging Time	0 hr	100 hr	1000 hr	2200 hr
Grain Size ASTM No.	6.9	6.8	6.9	6.8
Hardness Rockwell B	71	71	78	79

Table 3. Tensile properties of each aged specimen (* 0.2% offset yield strength)

Aging Time (hour)		0	100	1000	2200
Room Temp	Yield Strength* (MPa)	229.8	225.3	310.1	293.6
	Tensile Strength (MPa)	590.9	569.1	612.7	590.7
	Elongation(%)	51.7	48.1	42.2	46.5
	Reduction in Area (%)	77.6	66.2	50.4	48.7
650℃	Yield Strength* (MPa)	117.7	82.9	165.8	172.9
	Tensile Strength (MPa)	348.2	340.7	362.2	362.0
	Elongation(%)	29.0	24.4	37.5	28.9
	Reduction in Area.(%)	71.6	59.4	45.3	51.1

grain boundary and a few carbides in the grain. Fig. 3c is the microstructure of 1000 hr aged specimen at 750℃ and shows coarsened carbides in the grain and at the grain boundary. In case of 2200 hr aged specimen (Fig. 3d), more coarsened carbides were found in the whole grain and at the boundary. Laves phase and σ phase precipitates were not found with the light optical microscope.

Creep Rupture Test

Fig. 4 shows the creep elongation of the each aged specimen. Except 270MPa specimens, the creep elongation values increase significantly in 100 hr aged specimens followed by decrease in 1000 hr aged specimens and increase again in the 2200 hr specimens. This tendency is believed to be the result of easy glide motion of dislocations as the content of solutionized carbon decreases forming precipitates. The greatest elongation value of 100 hr aged specimens resulted from easier grain boundary sliding which was caused by finer carbides than those of 1000 hr and 2200 hr aged specimens. Comparing 1000 hr aged specimens with 2200 hr aged specimens, the elongation behavior can be explained by fracture modes. At the near failure surface of 1000 hr aged specimens, cavity type cracks grown transversely to the tensile direction were found. These cracks seem to grow to the critical size before significant elongation happens in the tensile direction. In 2200 hr aged specimens, cavity type cracks which were caused by carbides were found. The cavities that formed at the interface of the grain boundary carbides and grain boundary by grain boundary sliding grew into cracks along the grain boundary by continuous grain boundary sliding, and caused greater elongation in the tensile direction than that of 1000 hr aged specimens.

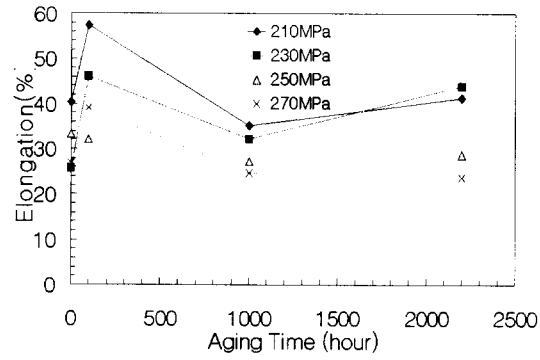

Fig. 4. Effect of aging time on creep ductility.

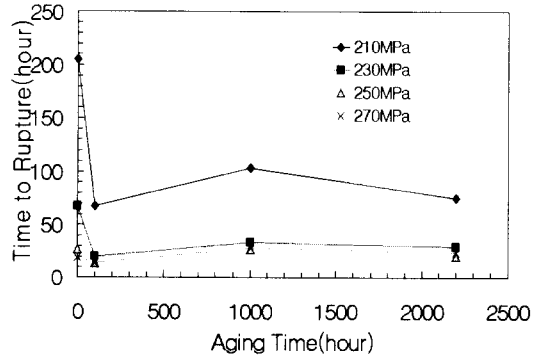

Fig. 5. Effect of aging time on time to rupture.

Fig. 5 shows the minimum creep rate of each

aged specimen. The 100 hr aged specimens showed the greatest rate and as the aging time gets longer, the rate decreased. The fine grain boundary carbides of 100 hr aged specimen made the grain boundary sliding easy, so the minimum creep rate increased. In case of 1000 hr and 2200 hr aged specimens, the coarsened grain boundary carbides made the grain boundary sliding difficult, and well dispersed carbides inside of the grains hindered the movement of dislocations.

Fig. 6 shows the time to rupture of each aged specimen. The rupture life of 100 hr aged specimen was the shortest. In case of 1000 hr aged specimen, the life increased a little, and in 2200 hr aged specimen, the life decreased again. Although the elongation was the greatest in 100 hr aged specimen, it had the shortest rupture life resulting from the fastest creep rate.

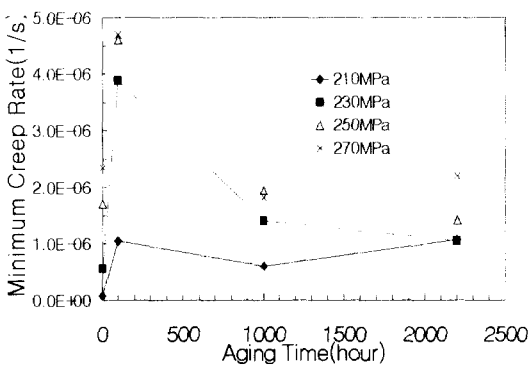

Fig. 6. Effect of aging time on minimum creep rate.

Fracture types were investigated with an optical microscope. Creep fracture types of all specimens were generally transgranular type fracture. In 1000 hr aged specimen, the cavity type microcracks were found at the interface of the carbide, which coarsened at grain boundary triple point. The microcracks grew transverse to the tensile direction. A triple point is a favorable site to precipitate and an early precipitated carbide coarsens the largest, and the carbide which becomes the stress concentration point offers crack initiation site. In 2200 hr aged specimen, cavitations occurred at grain boundary carbide interfaces and they coalesced. The coalescent cavities became microcracks and propagated along the grain boundaries. Nevertheless, the transgranular type fracture dominated over the cavity type fracture in both cases. Fig. 7 shows cavities in 1000 hr and 2200 hr aged specimens near the fracture surface.

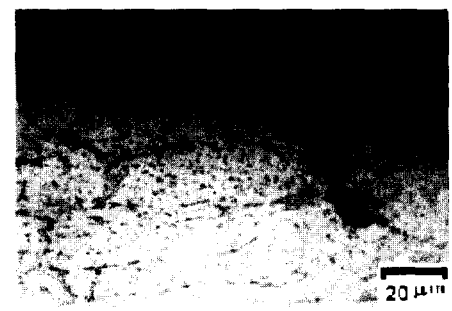

(a) 650℃/250MPa after 1000 hr aging

(b) 650℃/270MPa after 2200 hr aging

Fig. 7. Microstructures of ruptured specimen

Under the constant temperature, in the power law creep regime, the stress dependence of the minimum creep rate of stainless steel is expressed by an equation of the form[9].

$$\dot{\varepsilon}_m = A\sigma^n \qquad (1)$$

where $\dot{\varepsilon}_m$ is the minimum creep rate, A is a constant, σ is an applied stress, n is the creep

exponent. Each value of creep stress exponent, n, is determined by the same method shown in Fig. 8 for the case of not aged specimen. Fig. 9 shows the measured value of n of each aged specimen at 650℃.

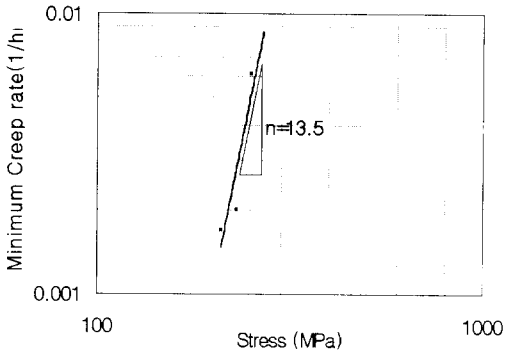

Fig. 8. Determination of the creep exponent n at 650℃. (not aged specimen)

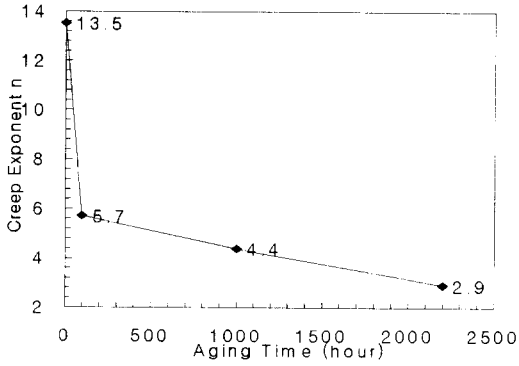

Fig. 9. Effect of aging time on the creep exponent n at 650℃

For the steady-state creep, the simplest assumption is that it is a singly activated process which can be expressed by an Arrhenius-type rate equation[10].

$$\dot{\varepsilon}_m = Be^{-\Delta H/RT} \qquad (2)$$

where $\dot{\varepsilon}_m$ is the minimum creep rate, B is a constant, R is the universal gas constant, T is the absolute temperature, and ΔH is the activation energy for the rate-controlling process. ΔH can be calculated by plotting $\ln \dot{\varepsilon}_m$ vs. 1/T which could be obtained through a set of tests with a small interval in temperature in order that creep mechanism may not change under the same stress condition.

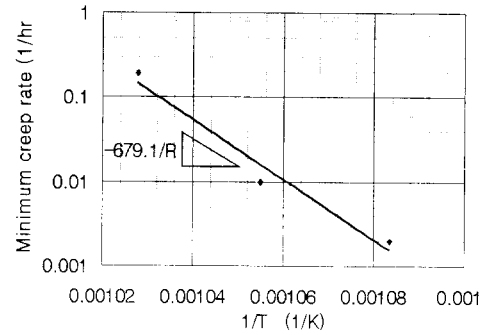

Fig. 10. Determination of creep activation energy ΔH. (not aged specimen)

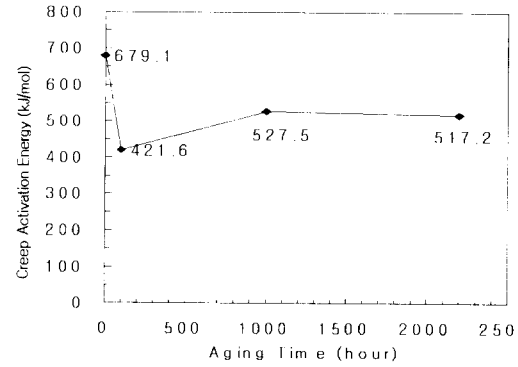

Fig. 11. Effect of aging time on the creep activation energy ΔH at 230MPa.

The value of each creep activation energy, ΔH, is obtained by the Arrhenius plot. Fig. 10 shows the determination of ΔH for the case of the specimen not aged. Fig. 11 shows the creep

activation energy of each aged specimen. The change of minimum creep rate vs. aging time can be explained by the value of the creep activation energy, i.e. as the creep activation energy gets greater, the minimum creep rate becomes slower because the creep deformation is constricted. In contrast, as the creep activation energy becomes smaller, the minimum creep rate becomes faster.

CONCLUSIONS

Using the prior aged 316 stainless steel, creep rupture tests were conducted under various stress conditions and at various temperatures. From the experimental results, following conclusions were obtained.

(1) The rupture life of 100 hr aged specimens was found to be the shortest, which is the result of the highest minimum creep rate. And the 0 hr aged specimens showed the longest rupture life, followed by 1000 hr aged and 2200 hr aged specimens.

(2) The value of the creep stress exponent, n, decreased as the aging time increased. The n values for the 0 hr, 100 hr, 1000 hr, 2200 hr aged specimens were measured to be 13.5, 5.7, 4.4 and 2.9.

(3) The creep activation energy varied with the aging time. The activation energies for 0 hr, 100 hr, 1000 hr and 2200 hr aged specimens were calculated to be 679.1, 421.6, 527.5 and 517.2 kJ/mol.

(4) The dominant fracture type of all aged specimens was the transgranular type fracture, but in 1000 hr and 2200 hr aged specimens, the cavity type microcracks were found at the interface of coarse carbide and grain boundary.

ACKNOWLEGEMENT

The authors are grateful for the support provided by a grant from the Korea Science & Engineering Foundation (KOSEF) and Safety and Structural Integrity Research Center at the Sungkyunkwan University.

REFERENCES

[1] Hong, S. H., and Yu, J., "Effect of Prior austenite grain size on creep properties and on creep crack growth in 3.5Ni-Cr-Mo-V steel", Scripta Metall., Vol. 23, p. 1057, 1989.

[2] Nakanishi, T., " A Study on the Effect of Helium Environment and the Grain Size on the Creep Behaviour of Hastelloy X alloy", JIM., Vol. 41, No. 3, p. 263, 1977.

[3] Choe, B. H., Kang, S. H. Lee, J. H., Choi, J. H. and Hur, B. Y., " Effect of the Carbide Behavior on Creep Properties of HK-40 Heat Resistant Steel", J. of the Korean Inst. of Met. & Mater., Vol. 35, No. 1, p. 23, 1997.

[4] Shinya, N., "Creep Rupture Properties and Creep Fracture Mechanism Maps for Type 304 Stainless Steel", ISIJ, Vol. 69, No. 14, p. 1668, 1983.

[5] Biss, V. A., "Metallographic Study of Type 304 Stainless Steel Long Term Creep-Rupture Specimen", Metall. Trans. A., Vol. 12A, p. 1360, 1981.

[6] Shinya, N., "Creep Fracture Mechanism Maps on Creep Rupture Test upto about 100000h for Type 316 Stainless Steel", ISIJ, Vol. 71, No. 1, p. 114, 1985.

[7] Kim, Y. S., Kim, S. E., Park, N. K., Kim, H. M., "Effect of Heat Treatment and HIPing on the Creep Properties of a Nickel Base Superalloy IN 713LC", J. of the Korean Inst. of Met. & Mater., Vol. 28, No. 10, p. 866, 1990.

[8] Shinya, N., " Creep Rupture Property and Microstructure Change in Type 316 Stainless Steel", Tetsu-to-Hagane, S1260, p. 206, 1982.

[9] Frost, H. J., Ashby, M. F., Deformation - Mechanism Maps, Pergamon Press, p.11, 1982.

[10] Dieter, G. E., Mechanical Metallugy, 3rd ed., McGraw -Hill, p. 450, 1988